Artificial Neural Network Approach to Single-Ended Fault Locator for Transmission Lines

Zhihong Chen, Jean-Claud Maun, Member, IEEE
Department of Electrical Engineering
Free University of Brussels(ULB)
B-1050, Brussels, Belgium

Abstract - **This paper describes the application of an artificial neural network-based algorithm to the single-ended fault location of transmission lines using voltage and current data. From the fault location equations, similar to the conventional approach, this method selects phasors of prefault and superimposed voltages and currents from all phases of the transmission line as inputs of the artificial neural network. The outputs of the neural network are the fault position and the fault resistance. With its function approximation ability, the neural network is trained to map the nonlinear relationship existing in the fault location equations with the distributed parameter line model. It can get both fast speed and high accuracy. The influence of the remote-end infeed on neural network structure is studied. A comparison with the conventional method has been done. It is shown that the neural network-based method can adapt itself to big variations of source impedances at the remote terminal. Finally, when the remote source impedances vary in small ranges, the structure of artificial neural network has been optimized by the pruning method.**

List of symbols

S, F, R : Sending (local) end, Fault point, and Receiving (remote) end.
A, B, C : phases of the three phase system.
0, 1, 2: Fortescue sequence components.
BF, DF, SUP : Prefault (Before Fault) state, During Fault state, and SUPerimposed state.
x : distance to fault from the sending end.
L : line Length.
R_f: fault resistance.
V, I : complex voltage and current phasors.
$\mathbf{Z}_{phase}$, $\mathbf{Y}_{phase}$: line impedance and admittance matrices in phase components.
p : phase index.
e : equivalent earth return index.
E, Z: Thévenin's equivalent of the external network.
W1, W2, b1, b2: weight matrixes and neuron bias vectors of layer 1 and 2 for the neural network.

I. INTRODUCTION

When a fault occurs on an electrical transmission line, it is very important to find the fault location in order to make necessary repairs and to restore power as soon as possible.

Many algorithms for accurate fault location have been developed. The algorithms based on the steady-state components at the fundamental frequency are still the most popular ones. Though the best way is to use all information from both terminals of the line [1] [2], which by principle can delete the influence of infeed current and fault resistance, most of fault locators are only based on the local measurement

The simplest single-ended fault location is the impedance based method like in a conventional distance relay [3]. Another approach is to use current distribution factors [4]. For long lines, a distributed parameter line model becomes essential for the design of an algorithm. Westlin et.al. [5] first introduced a methodology to incorporate this type of model for the determination of the fault distance. The Newton-Raphson method is applied to solve the related nonlinear equations. Unfortunately, due to the heavy computation burden of iterations, the equations are suggested to simplify to the short line model for the application. Moreover, Takagi et al. [6] used the superimposed components with the long line model. The fault current distribution factor is also introduced and assumed to be real. To avoid nonlinear optimization, this algorithm uses the Taylor expansion for hyperbolic functions. Recently, Johns et al. [7] proposed an algorithm directly using the condition that the fault admittance is real, but on-line nonlinear optimization is still necessary.

The modern trend of research, mainly for on-line application, is to get fast estimation and high accuracy

0-7803-3713-1/97 $10.00 © 1997 IEEE

simultaneously. The fault location equations based on the fundamental frequency components are strongly nonlinear, especially for the distributed parameter line model and therefore it is not easy, or even impossible, to obtain an analytical solution. Normally, iterative numerical methods should be applied. This is too slow for an on-line application. Moreover, some ill-conditions may occur [5]. For most of the existing algorithms, the complexity of the equations and the computation burden have to be reduced. Thus many influence factors can not be considered, such as shunt capacitance, line asymmetry, transposition points [14] , the change of the parameters along the line, and current transformer saturation.

Many successful applications of artificial neural networks to power system have been demonstrated including security assessment, load forecasting, control etc.. Recent applications in protection have covered fault direction discrimination, fault type classification, fault area estimation, autoreclosure technique, and transformer protection [8-13]. However, almost all these applications in protection merely use the ANN ability of classification, that is, ANNs only output 1 or 0, and the inputs are usually voltages and currents samples.

In this paper, a new ANN-based algorithm for the single-ended fault locator is proposed for on-line application. This method selects phasors of prefault and superimposed voltages and currents from all phases of the transmission line as the inputs of the ANN, and can output fast and accurate results, avoiding real-time nonlinear optimization. In addition, if necessary, many factors, which are not easy to consider with conventional methods, can be taken into account into the ANN.

II. BACKGROUND OF THE RESEARCH

A. System

The studied system is a two-busbar system shown in Fig. 1.

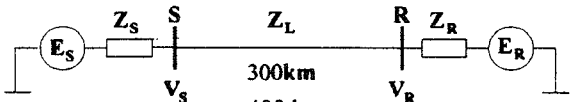

Fig. 1. Studied system.

The line is vertical arranged and untransposed. Its series impedance and shunt admittance matrices in phase components are given in Appendix.

B. Assumptions on the operation conditions:

Since the prefault conditions are used for the fault location based on the ANN, we assume :

- The prefault conditions are normal steady-state ones.
- The source impedances at both ends are symmetrica and remain the same before and during fault.
- The voltage amplitude at the busbars (V_S and V_R in Fi 1) is in the range [1.1 pu, 0.9 pu] and the angle betwee the busbar voltages is in the range [-20°, 20°].

C. Fault type and fault resistance

In the following, only the results for single phase to groun faults are presented. The fault resistance is assumed to b less than 20Ω.

D. Simulation cases:

Table 1. Typical source impedances

Source type	$\frac{\lvert Z_1\rvert}{\lvert Z_{Line}\rvert}$	angle(Z_1)	$\frac{\lvert Z_0\rvert}{\lvert Z_1\rvert}$	angle(Z_0) − angle(Z_1)
strong	0.08	89(°)	1.5	-1(°)
medium	0.3	87(°)	1	-3(°)
weak	1	85(°)	2	-5(°)

For all cases, the source at the sending end is always se weak. This is the worst condition for single-ended faul locators. At the receiving end, possible source impedance are strong, medium or weak.

All above data ranges are typical. The results will sho that they do not affect the principle of this method, only th size of the ANN.

III. BASIC EQUATIONS FOR SINGLE-ENDED FAULT LOCATION

To select the inputs of the ANN, we have first to analyz the basic equations for single-ended fault location. To give clear and simple description, basic equations are propose based on a phase symmetrical short-line model, since th distributed parameter line model is only applied to train an test the ANN, and the equations will not be solved. The sho line model can be described by only two parameters : th phase impedance Z_p, and the equivalent earth retur impedance Z_e, after eliminating the mutual coupling.

The principle of superimposition allows the faulted syste circuit to be decomposed into a prefault and a superimpose circuits, which are shown in Fig.2 for BG fault.

From Fig. 2, we can develop the basic equations for single end fault location. During the fault:

$$V_{s,DF,B} = x * Z_{L_p} * I_{s,DF,B} + R_f * I_f + x * Z_{L_e} * I_{s,DF,e} \quad (1)$$

In the superimposed state:

$$V_{s,SUP,B} = (L * Z_{L_p} + Z_{R_p}) * I_{s,SUP,B} + (L * Z_{L_e} + Z_{R_e}) * I_{s,SUP,e} - [(L - x) * Z_{L_p} + Z_{R_p} + (L - x) * Z_{L_e} + Z_{R_e}] * I_f \quad (2)$$

$$V_{S,SUP,A} = (L*Z_{L_p} + Z_{R_p})*I_{S,SUP,A} + (L*Z_{L_e} + Z_{R_e})*I_{S,SUP,e} - [(L-x)*Z_{L_e} + Z_{R_e}]*I_F \quad (3)$$

$$V_{S,SUP,C} = (L*Z_{L_p} + Z_{R_p})*I_{S,SUP,C} + (L*Z_{L_e} + Z_{R_e})*I_{S,SUP,e} - [(L-x)*Z_{L_e} + Z_{R_e}]*I_F \quad (4)$$

Under symmetrical conditions, (3) and (4) are redundant.

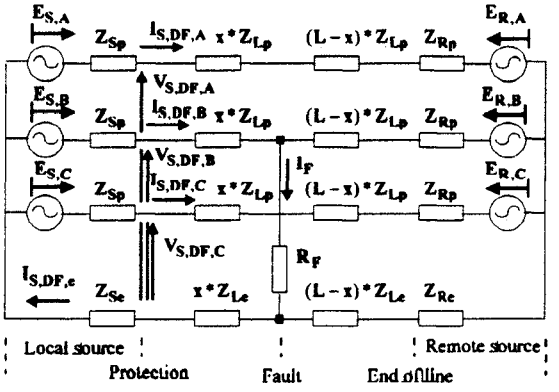

(a)

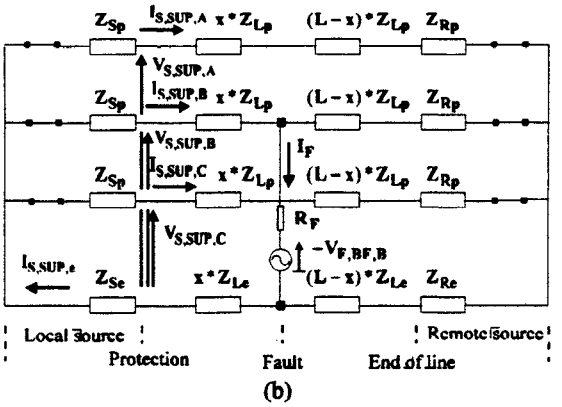

(b)

Fig. 2.The faulted (a) and superimposed (b) circuits for BG fault.

If the remote source impedances Z_{R_p} and Z_{R_e} are known, there are 6 independent real equations (3 complex equations based on (1), (2) and (3)) with 4 unknowns (x, R_f, and real and imaginary parts of I_F). The required information to solve equations are the phasors : $V_{S,DF,B}, I_{S,DF,B}, I_{S,DF,e}, V_{S,SUP,A}, V_{S,SUP,B}, I_{S,SUP,A}, I_{S,SUP,B}, I_{S,SUP,e}$

The equations are nonlinear even for the short line model. Compared with the ones using a distributed parameter line model [5], the relationship between the earth return currents of two terminals can not be deleted. This remaining correlation may increase the possibility of ill-conditions if we try to solve the equations iteratively.

IV. SINGLE-ENDED FAULT LOCATION BASED ON ANN

A. Inputs and outputs

To keep the symmetry for all single phase to ground faults, we use following inputs :

$V_{S,BF,A}, I_{S,BF,A}, V_{S,SUP,A}, V_{S,SUP,B}, V_{S,SUP,C}, I_{S,SUP,A}, I_{S,SUP,B}, I_{S,SUP,C}$

This means all information on three phases for the superimposed condition is input to the ANN, while only the information on phase A is used as the reference for the prefault condition.

There are 8 complex variables as input. If the prefault voltage is selected as the vector reference, the number of real variables can be reduced to 15. Normally, the interesting outputs are the fault distance x and the fault resistance R_f.

B. Architecture

The three layer feed-forward neural network is selected to implement the algorithm for the single-ended fault location. While the transfer function of the hidden layer neurons is the tanh function, in the output layer we use the linear function. This architecture has been proven to be an universal approximator [15].

Since the desired inputs of ANN for the single-ended fault location are the voltage and current phasors, which are complex values, we split them into real and imaginary parts and use a real feed-forward neural network. The complete structure of the ANN for the single-ended fault location is shown in Fig.3.

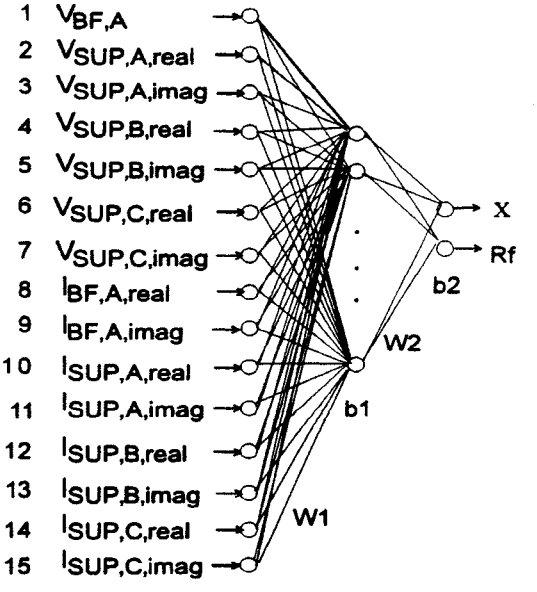

Fig. 3. ANN architecture for the single-ended fault location.

C. Learning rule

An improved batch backpropagation learning rule based on Levenberg-Marquardt optimization technique is used to train ANN. It is very powerful, but needs a lot of memory.

V. RESULTS

A. Division an ANN to a set of sub-ANNs according to the measured prefault condition at the local terminal

To get good general performance, for the single-ended fault location, the training and testing data have to cover wide system and fault conditions, e.g. prefault load, fault location and fault resistance. However, the more complex function to fit, the bigger the necessary size of the ANN. To avoid this problem, we can divide an ANN into a set of sub-ANNs according to the measured prefault condition at the local end. However, the bus voltages at the remote end is still considered in the wide range assumed in II.B.

B. Effect of different source impedances

The ANN training and testing for different remote source impedances have been done, according to the conditions in Table 1. Division of an ANN to a set of sub-ANNs based on the measured prefault condition at the local end is used. The results listed in Table 2 and 3 are given only under the conditions that the prefault real power through the line flows from the receiving end to the sending end, and that $1.0\text{pu.} \le \text{amplitude}(\mathbf{V}_s) \le 1.1\text{pu.}$.

Table 2. Results of ANNs for fault distance error(%)

Remote source	Hidden nodes	Data type	Maximum absolute	Mean	Standard deviation
Strong	12	Train	0.376	-0.0007	0.0961
		Test	1.003	0.0151	0.105
Medium	11	Train	0.123	-0.0002	0.036
		Test	0.125	-0.0092	0.031
Weak	8	Train	0.084	0.0000	0.021
		Test	0.265	0.0677	0.133

Table 3. Results of ANNs for fault resistance error(%)

Remote source	Hidden nodes	Data type	Maximum absolute	Mean	Standard deviation
Strong	12	Train	0.497	-0.0045	0.120
		Test	1.657	-0.1543	0.215
Medium	11	Train	0.251	0.0022	0.055
		Test	0.581	-0.1459	0.140
Weak	8	Train	0.202	0.0003	0.034
		Test	3.009	0.872	1.651

For each of the three remote source impedances, 5 training data and 4319 testing data are generated random The number of iterations for the training is 1000.
From these results, we can find :

- In all cases, the single-ended fault location based ANN can estimate the fault position with less than 1 error, and the fault resistance errors are smaller than 3 By principle, more accurate results may be obtained increasing the number of training data.
- Generally the more strong the possible influence of t remote source infeed is, the more complex t approximated function, and then the more nodes in t hidden layer are necessary. For this test, the difference small when the remote source is strong or medium.
- Though the results are the best compared with oth neural network structures with different hidden nodes, seems that, when the remote source is also weak, t ANN still overfits a little, suggesting that, there are little bit too many weights(hidden nodes) in the netwo [15].

A comparison with the conventional method can be do under the same conditions. Normally it is difficult to app nonlinear optimization for on-line application based on t basic single-ended fault location equations. Furthermore, the next section, the behavior for a range of remote sour impedances will be checked. However, almost conventional algorithms based on nonlinear optimizati need the remote source impedances as the settings. There no ability to adapt themselves to a large change of the remo source impedances. So a simpler and non-iterative metho which considers the fault current flowing the fault resistan to be proportional to the zero-sequence current at t protection for single-phase to ground faults, is selected. T equation for a BG fault is :

$$\mathbf{V}_{s,DF,B} = (\mathbf{Z}_{phase}(2,1) * \mathbf{I}_{s,DF,A} + \mathbf{Z}_{phase}(2,2) * \mathbf{I}_{s,DF,B} + \mathbf{Z}_{phase}(2,3) * \mathbf{I}_{s,DF,C}) * x + \mathbf{R}_F * 3\mathbf{I}_{s,DF,0} \quad (5)$$

The results for fault distance are listed in Table 4.

Table 4. Results of the conventional method for fault distance error(%)

Data type	Remote source	Maximum absolute	Mean	Standard deviation
Train	strong	340.310	-10.193	37.613
	medium	33.276	-2.297	3.864
	weak	2.030	-0.076	0.492
Test	strong	753.882	-3.261	20.663
	medium	30.334	-1.500	2.071
	weak	1.994	-0.193	0.337

It can be found that when the remote-end infeed is stron and the fault is near the remote end with large fa

resistance, the conventional method leads to very large errors. Only on-line nonlinear optimization can improve it.

In contrast to the conventional method, the influence of the remote-end infeed on the results of the ANN is not so apparent.

C. Adaptation to the change of source impedances

To check the ability of ANN to adapt itself to large variations of source impedances at the remote end, data for the three different types of remote sources have been used together to train an ANN.

As discussed above, for the phase symmetrical short line model, the nonlinear fault location equations are redundant if the remote end source impedances are known. However, when they are unknown, the nonlinear equations have eight unknowns for six equations and become under-determinated. Fortunately, under the following conditions, the methods still have opportunities to adapt themselves to the change of the source impedances at the remote end :

- Both $\mathbf{Z}_{Rp}$ and $\mathbf{Z}_{Re}$ change proportionally;
- Both $\mathbf{Z}_{Rp}$ and $\mathbf{Z}_{Re}$ are almost reactive;
- One of $\mathbf{Z}_{Rp}$ and $\mathbf{Z}_{Re}$ is fixed and the other varies.

For practical lines, if the geometry is not completely symmetrical, or the fault does not occur on the central phase of a line with a symmetrical geometry, the equations based on the healthy phases, (3) and (4), are slightly different, and more information can be given .

Though the remote source impedances in Table 1 do not completely fulfill one of the above conditions, an ANN is still trained and tested based on the data from three different types of remote sources together. Division of an ANN to a set of sub-ANNs is used, too. The following results only cover the prefault conditions that $0° \le \text{angle}(\mathbf{V}_R - \mathbf{V}_S) \le 20°$ and $1.05\text{pu} \le \text{amplitude}(\mathbf{V}_S) \le 1.1\text{pu}$.

The number of training data for each type of source is 1080, testing data are 3000. There are 27 nodes in the hidden layer. The number of training iterations is 300.

Table 5: Results of ANN for fault distance error(%), when remote source impedances change

Data type	Remote source	Maximum absolute	Mean	Standard deviation
Train	strong	1.411	0.0031	0.269
	medium	1.089	0.0007	0.225
	weak	0.773	-0.0009	0.200
	all	1.411	0.0010	0.233
Test	strong	3.545	0.0044	0.359
	medium	0.934	-0.0257	0.218
	weak	0.836	0.0274	0.196
	all	3.545	0.0020	0.269

Table 6: Results of ANN for fault resistance error(%), when the remote source impedances change

Data type	Remote source	Maximum absolute	Mean	Standard deviation
Train	strong	1.746	-0.006	0.387
	medium	1.671	-0.015	0.349
	weak	1.415	-0.004	0.353
	all	1.746	-0.008	0.363
Test	strong	29.844	0.100	2.199
	medium	17.706	0.094	1.254
	weak	2.152	-0.061	0.564
	all	29.844	0.043	1.499

The results show that, when the source impedances at the remote end vary in a large range, the ANN is able to make the internal decision to know which source is practically in operation. Then the fault distance is given based on this decision. The observed maximum absolute error for fault distance is 3.5%.

D. Small range changes of source impedances and ANN strucrure optimization

A more practical condition is to assume that the source impedances change continually in small ranges. Since the influence of the local source is small, still only the remote source impedances are considered. The remote source is assumed as a medium source in Table 1 with ±5% deviation for the amplitudes of the sequence impedances and ±1° deviation for the angles of sequence impedances.

For this test, the structure of the ANN is optimized with the *optimal brain damage* method [15] to get better generalization and a smaller architecture. At first a relatively large initial network is trained with little overfitting for the testing data. Then some unnecessary weights are pruned depending on their sensitivity to the estimation error. After retraining the ANN and repruning the weights, the optimal architecture can be found with the smallest mean square error for the testing data.

To show the results more clearly, the outputs of the ANN are reduced to the fault position only.

Using the division of an ANN to a set of sub-ANNs based on the measured prefault condition at the local end, the prefault system conditions for the following results are only $0° \le \text{angle}(\mathbf{V}_R - \mathbf{V}_S) \le 20°$ and $1.0\text{pu} \le \text{amplitude}(\mathbf{V}_S) \le 1.1\text{pu}$.

The number of training data is 2515 including 512 boundary points. The test data are 2000.

The initial network has 25 nodes in hidden layer and is trained by 2000 iterations. Each time 2% of the weights are pruned and the network is retrained with 25 iterations.

Table 7 and 8 show the results before and after pruning when the optimal structure has been obtained.

Table 7 Comparison of the network structure and performance between before and after pruning

	Hidden nodes	Number of weights	Data Type	Mean Square Error
Before pruning	25	426	Train	2.794E-5
			Test	7.856E-5
After pruning	18	227	Train	4.297E-5
			Test	6.837E-5

Table 8 Comparison of the fault distance error(%), among conventional method, before and after pruning

	Data Type	Maximum absolute	Mean	Standard deviation
Before pruning	Train	2.391	0.000	0.415
	Test	4.044	0.027	0.696
After pruning	Train	3.232	-0.001	0.515
	Test	3.720	0.022	0.649
Conventional method	Train	45.405	-2.149	4.330
	Test	24.231	-1.946	1.937

Before pruning the results for the testing data are not as good as for the training data. By comparison with other neural network structures with different hidden nodes, this initial network is known to little overfit [15], though it is the best in our initial try. After finding the optimal architecture by pruning, while the results for the training data become little worse, the results for the testing data are modified. The pruned network gets better generalization performance for the untrained data.

In addition, the pruned network has only 18 nodes in hidden layer with 227 weights. 46.7% of the weights and 7 nodes have been deleted. This leads easier realization and higher execution speed.

For the same network, a more complex pruning method, the *optimal brain surgeon* [15], which theoretically can delete the weights more accurately, was also tested. However, since the necessary network size must remain large and computation burden increases too much, no better result has been obtained.

Both above pruning methods treat the input nodes and the hidden nodes identically. It is helpful for automatic selection of input features. If all weights connected to an input are deleted after the optimum network has been found, it is conclusive that this input is not necessary for the considered problem. This ability is very important for some difficult protection problems [11][13], and is not easy to implement by conventional method and other ANN structure design methods.

VI. CONCLUSIONS

This paper has described an ANN-based single-ended fau location method. For on-line application, it can reach fa speed and high accuracy simultaneously, and give designe more opportunities to consider more factors, which are n easy to be treated by conventional methods. Th methodology has the ability of adapting itself to lar variations of remote source impedances.

The pruning method, *optimal brain damage*, is helpful get a network with better generalization performance. Tl designing process of an ANN has proven this when tl remote source impedances vary in small ranges. Its ability automatic selection will find application for other protectic problems.

All selected ranges of values have no influence on tl principle of this method, only on the size of the ANN. W can easily extend this method to very high resisti faults(e.g. 200 Ω), more general system configurations, ar even two-end fault locator. Furthermore, because of its fa response speed, it is also possible to use this ANN base method to the adaptive digital distance protection directly.

VII. ACKNOWLEDGMENT

We thank Dr. L.Philippot, Mr. D. Wiot and Mr. J.Coemar for valuable discussions. This research is supported b SIEMENS AG.

VIII. REFERENCES

[1] A.A.Girgis, D.G.Hart and W.L.Peterson, "A new fau location technique for two- and three-terminal lines", IEE *Trans. on Power Delivery*, Vol.7, No.1, 1992, pp.98-107.

[2] J.-C.Maun, L.Philippot, Z. Chen, and M. Mouvet, "Fau locator based on two-end measurement -and least-squar estimation", Southern African Power System Protectio Conference, Midrand , Nov., 1994.

[3] A.Wiszniewski, "Accurate fault impedance locatin algorithm", IEE Proc.C, Vol.130, No.6, 1983, pp.311-314.

[4] L.Eriksson, M.M.Saha and G.D.Rockefeller, "A accurate fault locator with compensation for apparer reactance in the fault resulting remote end infeed", IEE *Trans.*, Vol.PAS-104, No.1, 1985, pp. 424-436.

[5] S.E.Westlin and J.A.Bubenko, "Newton -Raphso technique applied to the fault location problem", IEEE PE Summer Meeting, 1976, Paper No. A 76 334-3.

[6] T.Takagi et al., "Development of a new type fault locat using the one-terminal voltage and current data", IEE *Trans.*, Vol. PAS-101, No.8, 1982, pp. 2892-2897.

[7] A.T.Johns, P.J.Moore and B.Whittard, "New techniq for the accurate location of earth faults on transmissic systems", IEE Proc.C, Vol.142, No.2, 1995, pp.119-127.

[8] T. S.Sidhu, H. Singh and M. S.Sachdev, "Desig implication and testing of an artificial neural network base

fault direction discriminator for protecting transmission lines", IEEE *Trans. Power Delivery*, Vol.10, No.2, 1995, pp. 697-706.

[9] T. Dalstein and B. Kulicke, "Neural network approach to fault classification for high speed protective relaying", IEEE *Trans. Power Delivery*, Vol.10, No.2, 1995, pp 1002-1011.

[10] T. Dalstein, T. Friedrich, B. Kulicke and D. Sobajic, "Multi neural network based fault area estimation for high speed protective relaying", IEEE *Trans. Power Delivery*, Vol.11, No.2, 1996, pp 740-747.

[11] R.K.Aggarwal, A.T.Johns, Y.Song, R.W.Dunn and D.S.Fitton, "Neural-network based adaptive single-pole autoreclosure technique for EHV transmission system", IEE Proc.C, Vol.141, No.2, 1994, pp.155-160.

[12] M.Kezunovic, I.Rikalo and D.J.Sobajic, "Neural Network applications to real-time and off-line fault analysis", Intl. Conf. on Intelligent System Applications to Power Systems, France, Sept. 1994.

[13] P.Bastard, M.Meunier, and H.Régal, "Neural network-based algorithm for power transformer differential relays", IEE Proc.C, Vol.142, No.4, 1995, pp.386-392.

[14] L.Philippot, Z. Chen, and J.-C.Maun, "Transmission system modeling requirements for testing high-accuracy fault locators", Proc. of 1st Intl. Conf. on Digital Power System Simulations, Texas, USA, Apr. 1995.

[15] C.M.Bishop, Neural Networks for Pattern Recognition, Oxford University Press Inc. New York,1995.

IX. APPENDIX

The series impedance and shunt admittance matrices in phase components obtained by the LINE CONSTANTS support routine of EMTP at 50 Hz, using the "K.C.Lee" untransposed line model.

$$Z_{phase} = \begin{bmatrix} 4.107778E-02 & & & \\ +j*4.46379E-01 & & & \\ 2.695538E-02 & 4.269062E-02 & & \\ +j*1.903961E-01 & +j*4.745678E-01 & & \\ 2.735199E-02 & 2.855895E-02 & 4.398963E-02 & \\ +j*1.617875E-01 & +j*2.215322E-01 & +j*4.853872E-01 & \end{bmatrix} \Omega/km$$

$$Y_{phase} = j* \begin{bmatrix} 1.058444E-08 & & \\ -2.415754E-09 & 1.131348E-08 & \\ -8.739274E-10 & -2.458611E-09 & 1.182518E-08 \end{bmatrix} S/km$$

X. BIOGRAPHY

Zhihong Chen was born in the People's Republic of China. He received the B.E. degree in information and Control Engineering, and M.Sc in Electrical Engineering in 1986 and 1989, respectively, from Xian Jiaotong University. He was a lecture in the department of Electrical Engineering of this university from 1989 to 1993. He has participated to several projects related to power system projection and control. He is now working at the Free University of Brussels(ULB) towards to Ph.D. His research interests include power system protection and control, signal processing and application of AI.

Jean-Claude Maun received the M.Sc in Mechanical and Electrical Engineering in 1976 and Ph.D. degree in Applied Science in 1981, both from the Free University of Brussels(ULB), Belgium. He joined the Electrical Engineering Department of ULB in 1976 and is now a professor. He has been leading research projects in the field of digital protections design for Siemens more than ten years. His research includes all aspects of power system protections, as well as the dynamic and control of synchronous machines